New York Journal of Mathematics

New York J. Math. **27** (2021) 124–140.

# Comparing Bennequin-type inequalities

**Elaina Aceves, Keiko Kawamuro and Linh Truong**

Abstract. The slice-Bennequin inequality gives an upper bound for the self-linking number of a knot in terms of its four-ball genus. The $s$-Bennequin and $\tau$-Bennequin inequalities provide upper bounds on the self-linking number of a knot in terms of the Rasmussen $s$ invariant and the Ozsváth-Szabó $\tau$ invariant. We exhibit examples in which the difference between self-linking number and four-ball genus grows arbitrarily large, whereas the $s$-Bennequin inequality and the $\tau$-Bennequin inequality are both sharp.

Contents



## 1. Introduction

In the standard contact 3-space $(\mathbb{R}^3, \xi_{\text{std}})$, knots that are transverse to the contact planes can be viewed as braids around the $z$-axis. In this paper we will view transverse knots by their braid representations. Let $B_n$ be the Artin braid group generated by $\sigma_1, \dots, \sigma_{n-1}$ with the relations

$$\sigma_i\sigma_j = \sigma_j\sigma_i \text{ for } |i-j| > 1$$
$$\sigma_i\sigma_{i+1}\sigma_i = \sigma_{i+1}\sigma_i\sigma_{i+1} \text{ for } i = 1, \dots, n-2.$$

Received September 25, 2020.

2010 *Mathematics Subject Classification.* 57K10.

*Key words and phrases.* slice Bennequin inequality, 4-ball genus, $\tau$-invariant, $s$-invariant, non-quasipositive knot.

EA was partially supported by the Ford Foundation. KK was partially supported by Simons Foundation Collaboration Grants for Mathematicians and NSF grant DMS-2005450. LT was partially supported by NSF grants DMS-200553 and DMS-2104309.

ISSN 1076-9803/2021

The self-linking number is an invariant of a transverse link. If a transverse knot is represented by a braid $\beta \in B_n$ then the self-linking number can be computed using the formula

$$sl(\widehat{\beta}) = -n + a,$$

where $\widehat{\beta}$ is the closure of $\beta$, $n$ is the braid index of $\beta$ and $a$ is the exponent sum of $\beta$ (or the algebraic crossing number of $\beta$). Given a topological knot type $K$ in $S^3$ we denote by $SL(K)$ the maximal value of the self-linking numbers of transverse knot representatives and call it *the maximal self-linking number* of $K$. Bennequin [Ben83] showed $sl(\widehat{\beta}) \leq 2g_3(K) - 1$ where $\beta$ is a braid representative of $K$ and $g_3(K)$ denotes the genus of the knot type $K$; thus,

$$SL(K) \leq 2g_3(K) - 1.$$

The knot invariants we examine in this paper include the maximal self-linking number $SL(K)$, the four ball genus $g_4(K)$, the Ozsváth-Szabó concordance invariant $\tau(K)$ [OS03], and the Rasmussen concordance invariant $s(K)$ [Ras10]. We also consider the transverse invariants $\hat{\theta}(K)$ [OST08] from Heegaard Floer homology and $\psi(K)$ [Pla06] from Khovanov homology.

For any knot type $K$, we have the following bounds on the self-linking number:

$$SL(K) \leq s(K) - 1 \leq 2g_4(K) - 1 \leq 2g_3(K) - 1.$$

Rudolph [Rud93] proved $SL(K) \leq 2g_4(K) - 1$. Plamenevskaya [Pla06], Shumakovitch [Shu07], and Kawamura [Kaw07] proved the first inequality $SL(K) \leq s(K) - 1$. Rasmussen defined the $s$ invariant and proved that $s(K) \leq 2g_4(K)$ in [Ras10] which gives us the second inequality. In [Par12], Pardon extended the $s$ invariant from knots to links. Plamenevskaya's proof still applies with Pardon's definition, so we have a bound for the self-linking number.

The concordance invariant $\tau(K)$ defined using Heegaard Floer homology [OS03] gives similar bounds [OS03, Pla04]:

$$SL(K) \leq 2\tau(K) - 1 \leq 2g_4(K) - 1 \leq 2g_3(K) - 1.$$

**Definition 1.1** ([HIK19])**.** Let $K$ be a knot type in $S^3$. The *defect of the slice-Bennequin inequality* is defined as

$$\delta_4(K) = \frac{1}{2}(2g_4(K) - 1 - SL(K)).$$

**Definition 1.2.** Let $K$ be a knot type in $S^3$. We define the *defect of the $s$-Bennequin inequality* as

$$\delta_s(K) = \frac{1}{2}(s(K) - 1 - SL(K)),$$

and the *defect of the $\tau$-Bennequin inequality* as

$$\delta_\tau(K) = \frac{1}{2}(2\tau(K) - 1 - SL(K)).$$

Note that the defects $\delta_4$, $\delta_s$, and $\delta_\tau$ are always nonnegative.

In our main result, we show that the defect $\delta_4(K)$ can be made arbitrarily large, while at the same time the defects $\delta_s(K)$ and $\delta_\tau(K)$ are both bounded.

**Theorem 1.3.** *There exists a family of knots $K_n$, where $n = 1, 2, \ldots,$ such that $\delta_4(K_n) = 2n$, whereas $\delta_s(K_n) = 0$ and $\delta_\tau(K_n) = 0$.*

We give the first example of such an infinite sequence in the literature.

Any knot satisfying Theorem 1.3 must be non-quasipositive. However, we will show in Section 2.5 that the non-quasipositive property of the knots $K_n$ is not detected by the Ozsváth-Szabó-Thurston transverse invariant $\hat{\theta}(K)$ from knot Floer homology [OST08] and Plamenevskaya's $\psi(K)$ from Khovanov homology [Pla06].

**Definition 1.4.** A braid $\beta \in B_n$ is *quasipositive* if it is a product of positive powers of some conjugates of the standard generators $\sigma_1, \ldots, \sigma_{n-1}$. In other words, $\beta$ is quasipositive if it is conjugate to a braid word of the form

$$(w_1\sigma_{i_1}w_1^{-1})(w_2\sigma_{i_2}w_2^{-1})\cdots(w_k\sigma_{i_k}w_k^{-1})$$

for some braid words $w_1, \ldots, w_k$. A knot or link is then *quasipositive* if it can be represented by a quasipositive braid.

We have the following result when $K$ is quasipositive.

**Proposition 1.5.** If $K$ is a quasipositive knot, then we have

$$\delta_s(K) = \delta_\tau(K) = \delta_4(K) = 0.$$

**Proof.** Let $K$ be quasipositive. Plamenevskaya [Pla04] and Hedden [Hed10] proved the equality $SL(K) = 2\tau(K) - 1$, and Plamenskaya [Pla06] and Shumakovitch [Shu07] proved the equality $SL(K) = s(K) - 1$. That the defect of the slice-Bennequin inequality of a quasipositive knot vanishes is well-known (see, for example, [HIK19, Proposition 1.10]). $\square$

**Acknowledgements.** The authors would like to thank Gage Martin and Matt Hedden for useful conversation, and the anonymous referee for numerous comments.

## 2. A sequence of non-quasipositive braids

Throughout the rest of this paper, we focus on a particular sequence of braids and their knot closures. For each $n = 1, 2, \ldots,$ we define the 3-stranded braid $\beta_n$ as

$$\beta_n = (\sigma_1^{-1})^{2n+3}\sigma_2(\sigma_1)^3\sigma_2.$$

The braid closure of $\beta_n$ is a knot denoted by $K_n = \widehat{\beta_n}$. The braid $\beta_n$ is shown in Figure 1.

**Theorem 2.1.** *For each $n = 1, 2, \ldots,$ let $K_n$ be the knot constructed above. The defect of the slice Bennequin inequality for the knot $K_n$ is $\delta_4(K_n) = 2n$. On the other hand, $\delta_s(K_n) = 0$ and $\delta_\tau(K_n) = 0$.*

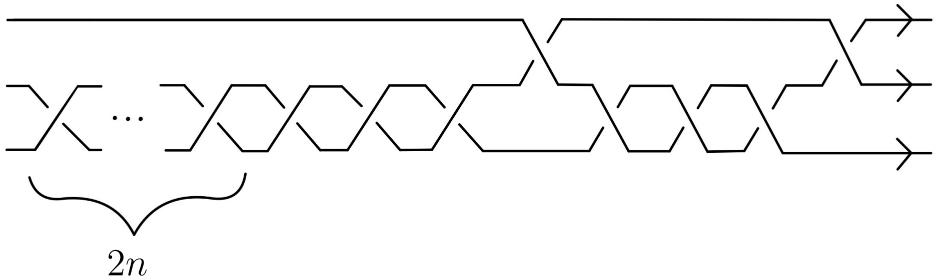


FIGURE 1. The braid $\beta_n$. The braid closure $K_1 = \widehat{\beta_1}$ is the knot $10_{125}$ and $K_2 = \widehat{\beta_2}$ is the knot $12n235$.

Theorem 1.3 from the Introduction follows from Theorem 2.1.

The proof of Theorem 2.1 will rely on the signature bound on the four-ball genus: $\frac{1}{2}\sigma(K) \leq g_4(K)$. For the knots $K_n$, this signature bound will prove to be stronger than the $s$-invariant bound $\frac{1}{2}s(K) \leq g_4(K)$ and the $\tau$-invariant bound $\tau(K) \leq g_4(K)$.

**Proof of Theorem 2.1.** The result will follow from Corollary 2.7, Proposition 2.9, and Proposition 2.10. □

**2.1. Signature of $K_n$.** The goal of this section is to prove that the signature of $K_n$ is $2n$.

We begin with the case $n = 1$. Figure 2 shows a Seifert surface $T_1$ with oriented boundary $K_1$. The Euler characteristic of $T_1$ is

$$\chi(T_1) = 3 - 8 = -5.$$

That is, the surface $T_1$ has genus 3. The oriented curves $\gamma_1, \ldots, \gamma_6$ shown in Figure 2 generate the homology group $H_1(T_1) \simeq \mathbb{Z}^6$. Let $\gamma_j^+$ be the push-off of $\gamma_j$ in the positive normal direction of the surface. Since the Seifert matrix, $V_1$, has $(i,j)$-entries $lk(\gamma_i, \gamma_j^+)$ we have

$$V_1 = \begin{pmatrix} -2 & 0 & -1 & 0 & 0 & 0 \\ -1 & -1 & 0 & 0 & 0 & 0 \\ 0 & 1 & 0 & -1 & 0 & 0 \\ 0 & 0 & 0 & 1 & -1 & 0 \\ 0 & 0 & 0 & 0 & 1 & -1 \\ 0 & 0 & 0 & 0 & 0 & 1 \end{pmatrix}.$$

**Lemma 2.2.** The signature of $K_1$ is $\sigma(K_1) = 2$.

We show detailed computation since this will play the base case of the induction step to compute the signature of general $K_n$.

**Proof.** The signature $\sigma(K_1)$ is the number of positive eigenvalues of $V_1 + V_1^T$ minus the number of negative eigenvalues of $V_1 + V_1^T$, where $V_1^T$ denotes the transpose of $V_1$.

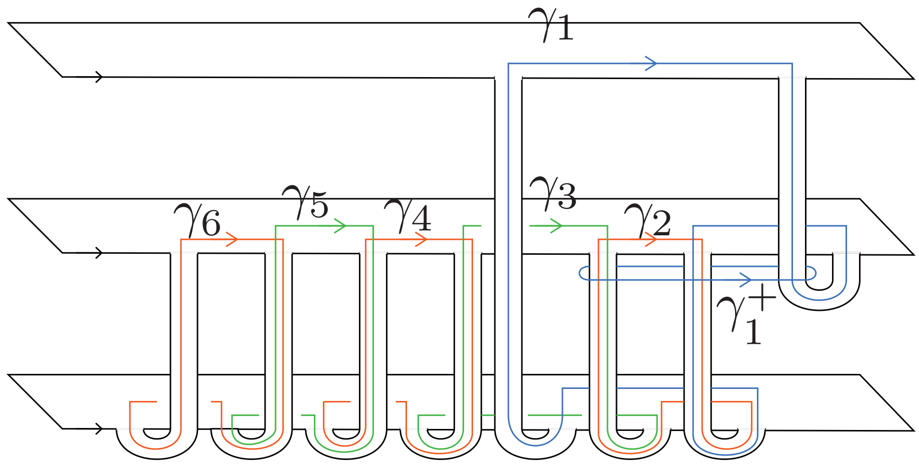


FIGURE 2. The Seifert surface $T_1$ of $K_1$. The oriented curves $\gamma_1, \ldots, \gamma_6$ generate the homology group $H_1(T_1)$. The pushoff $\gamma_1^+$ links with other curves.

After performing the row operations to $V_1 + V_1^T$ detailed in Figure 3, we arrive at a row reduced matrix with two negative diagonal entries and four positive diagonal entries. Thus, $\sigma(K_1) = 4 - 2 = 2$. $\square$

We can generalize the construction of the Seifert surface for $K_1$ to create for each $n \geq 2$ a Seifert surface $T_n$ for $K_n$ shown in Figure 4. The box $B(n)$ represents $2n-3$ negative bands between the bottom two disks. The oriented curves $\gamma_1, \ldots, \gamma_{2n+4}$ generate $H_1(T_n)$. The curves $\gamma_6, \ldots, \gamma_{2n-2}$, which encircle adjacent bands (similar to $\gamma_4, \gamma_5$ and $\gamma_6$ from Figure 2), as well as the other half of the curves $\gamma_5$ and $\gamma_{2n+3}$ are not drawn but are also represented by the box. All of the curves are oriented in the same direction, namely oriented clockwise. The associated Seifert matrix $V_n$ and the symmetric matrix $V_n + V_n^T$ have size $(2n+4) \times (2n+4)$ and are given below.

$$V_n = \left(\begin{array}{cccc|cccc}
-2 & 0 & -1 & 0 & & & & \\
-1 & -1 & 0 & 0 & & & \mathbf{0} & \\
0 & 1 & 0 & -1 & & & & \\
0 & 0 & 0 & 1 & -1 & & & \\
\hline
 & & & & 1 & -1 & & \\
 & & & & & 1 & & \\
 & & \mathbf{0} & & & & \ddots & \\
 & & & & & & & -1 \\
 & & & & & & & 1
\end{array}\right)$$

$$V_1 + V_1^T = \begin{pmatrix} -4 & -1 & -1 & 0 & 0 & 0 \\ -1 & -2 & 1 & 0 & 0 & 0 \\ -1 & 1 & 0 & -1 & 0 & 0 \\ 0 & 0 & -1 & 2 & -1 & 0 \\ 0 & 0 & 0 & -1 & 2 & -1 \\ 0 & 0 & 0 & 0 & -1 & 2 \end{pmatrix}$$

$$\xrightarrow{\text{Step 1}} \begin{pmatrix} -4 & -1 & -1 & 0 & 0 & 0 \\ 0 & -7/4 & 5/4 & 0 & 0 & 0 \\ 0 & 5/4 & 1/4 & -1 & 0 & 0 \\ 0 & 0 & -1 & 2 & -1 & 0 \\ 0 & 0 & 0 & -1 & 2 & -1 \\ 0 & 0 & 0 & 0 & -1 & 2 \end{pmatrix} \qquad \begin{array}{l} R_2 \to R_2 - \frac{1}{4}R_1 \\ R_3 \to R_3 - \frac{1}{4}R_1 \end{array}$$

$$\xrightarrow{\text{Step 2}} \begin{pmatrix} -4 & 0 & -12/7 & 0 & 0 & 0 \\ 0 & -7/4 & 5/4 & 0 & 0 & 0 \\ 0 & 0 & 8/7 & -1 & 0 & 0 \\ 0 & 0 & -1 & 2 & -1 & 0 \\ 0 & 0 & 0 & -1 & 2 & -1 \\ 0 & 0 & 0 & 0 & -1 & 2 \end{pmatrix} \qquad \begin{array}{l} R_1 \to R_1 - \frac{4}{7}R_2 \\ R_3 \to R_3 + \frac{5}{7}R_2 \end{array}$$

$$\xrightarrow{\text{Step 3}} \begin{pmatrix} -4 & 0 & 0 & -3/2 & 0 & 0 \\ 0 & -7/4 & 0 & 35/32 & 0 & 0 \\ 0 & 0 & 8/7 & -1 & 0 & 0 \\ 0 & 0 & 0 & 9/8 & -1 & 0 \\ 0 & 0 & 0 & -1 & 2 & -1 \\ 0 & 0 & 0 & 0 & -1 & 2 \end{pmatrix} \qquad \begin{array}{l} R_1 \to R_1 + \frac{3}{2}R_3 \\ R_2 \to R_2 - \frac{35}{32}R_3 \\ R_4 \to R_4 + \frac{7}{8}R_3 \end{array}$$

$$\xrightarrow{\text{Step 4}} \begin{pmatrix} -4 & 0 & 0 & 0 & -4/3 & 0 \\ 0 & -7/4 & 0 & 0 & 35/36 & 0 \\ 0 & 0 & 8/7 & 0 & -8/9 & 0 \\ 0 & 0 & 0 & 9/8 & -1 & 0 \\ 0 & 0 & 0 & 0 & 10/9 & -1 \\ 0 & 0 & 0 & 0 & -1 & 2 \end{pmatrix} \qquad \begin{array}{l} R_1 \to R_1 + \frac{4}{3}R_4 \\ R_2 \to R_2 - \frac{35}{36}R_4 \\ R_3 \to R_3 + \frac{8}{9}R_3 \\ R_5 \to R_5 + \frac{8}{9}R_5 \end{array}$$

$$\xrightarrow{\text{Step 5}} \begin{pmatrix} -4 & 0 & 0 & 0 & 0 & -6/5 \\ 0 & -7/4 & 0 & 0 & 0 & 7/8 \\ 0 & 0 & 8/7 & 0 & 0 & -4/5 \\ 0 & 0 & 0 & 9/8 & 0 & -9/10 \\ 0 & 0 & 0 & 0 & 10/9 & -1 \\ 0 & 0 & 0 & 0 & 0 & 11/10 \end{pmatrix} \qquad \begin{array}{l} R_1 \to R_1 + \frac{6}{5}R_5 \\ R_2 \to R_2 - \frac{7}{8}R_5 \\ R_3 \to R_3 + \frac{4}{5}R_5 \\ R_4 \to R_4 + \frac{9}{10}R_5 \\ R_6 \to R_6 + \frac{9}{10}R_5 \end{array}$$

$$\xrightarrow{\text{Step 6}} \begin{pmatrix} -4 & 0 & 0 & 0 & 0 & 0 \\ 0 & -7/4 & 0 & 0 & 0 & 0 \\ 0 & 0 & 8/7 & 0 & 0 & 0 \\ 0 & 0 & 0 & 9/8 & 0 & 0 \\ 0 & 0 & 0 & 0 & 10/9 & 0 \\ 0 & 0 & 0 & 0 & 0 & 11/10 \end{pmatrix} \qquad \begin{array}{l} R_1 \to R_1 + \frac{12}{11}R_6 \\ R_2 \to R_2 - \frac{35}{44}R_6 \\ R_3 \to R_3 + \frac{8}{11}R_6 \\ R_4 \to R_4 + \frac{9}{11}R_6 \\ R_5 \to R_5 + \frac{10}{11}R_6 \end{array}$$

FIGURE 3. We denote the $i$th row in the matrix as $R_i$, and denote by $R_i \to R_i + cR_j$ with $c \in \mathbb{Q}$ the row operation replacing the row $R_i$ with $R_i + cR_j$.

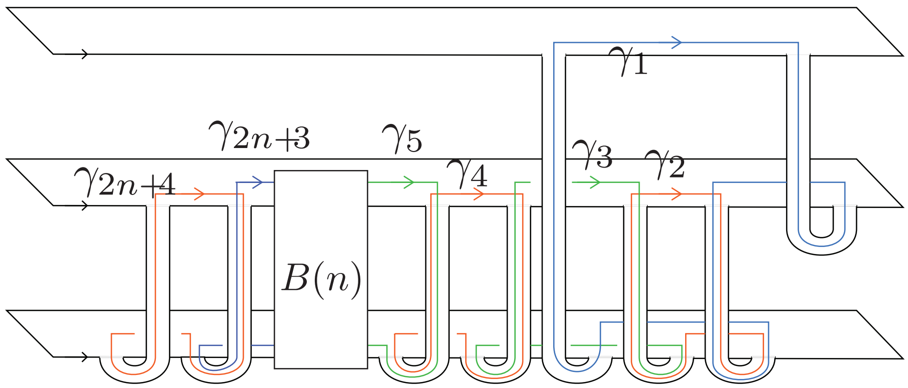


FIGURE 4. The Seifert surface $T_n$ of $K_n$. The oriented curves $\gamma_1, \ldots, \gamma_{2n+4}$ generate $H_1(T_n)$.

$$V_n + V_n^T = \left(\begin{array}{ccc|ccccc} -4 & -1 & -1 & & & & & \\ -1 & -2 & 1 & & & & 0 & \\ -1 & 1 & 0 & -1 & & & & \\ \hline & & -1 & 2 & -1 & & & \\ & & & -1 & 2 & & & \\ & 0 & & & & \ddots & & \\ & & & & & & & -1 \\ & & & & & & -1 & 2 \end{array}\right)$$

Let $M_1 = V_1 + V_1^T$. We inductively define the matrices $M_n$ of size $(n+5) \times (n+5)$ for $n = 1, 2, \ldots$ as follows.

$$M_1 = \left(\begin{array}{ccc|ccc} -4 & -1 & -1 & 0 & 0 & 0 \\ -1 & -2 & 1 & 0 & 0 & 0 \\ -1 & 1 & 0 & -1 & 0 & 0 \\ \hline 0 & 0 & -1 & 2 & -1 & 0 \\ 0 & 0 & 0 & -1 & 2 & -1 \\ 0 & 0 & 0 & 0 & -1 & 2 \end{array}\right) \qquad M_n = \left(\begin{array}{ccc|c} & M_{n-1} & & \begin{matrix} 0 \\ \vdots \\ 0 \\ -1 \end{matrix} \\ \hline 0 & \cdots & 0 \;\; -1 & 2 \end{array}\right)$$

Observe that $M_{2n-1} = V_n + V_n^T$. The signature of the knot $K_n$ is the signature of the matrix $M_{2n-1}$, which can be computed with the help of the following lemma.

**Lemma 2.3.** We can reduce $M_n$ to the matrix $\widetilde{M_n}$ using only row operations in the first $n+4$ rows where an asterisk designates that the entry could be any rational number.

$$\widetilde{M}_n = \left(\begin{array}{ccccccc} -4 & 0 & & & & & * \\ 0 & -7/4 & & & 0 & & * \\ & & 8/7 & & & & * \\ & & & 9/8 & & & \vdots \\ & 0 & & & \ddots & & * \\ & & & & & \frac{n+9}{n+8} & -1 \\ & & & & & -1 & 2 \end{array}\right)$$

**Proof.** We will prove this by induction on $n$.

We have already shown that $M_1$ can be reduced to $\widetilde{M}_1$ using row operations in the first five rows by following Steps 1-4 and the first four row operations from Step 5 in Figure 3. Hence the base case is satisfied.

$$\widetilde{M}_1 = \left(\begin{array}{cccccc} -4 & 0 & & 0 & & -6/5 \\ 0 & -7/4 & & & & 7/8 \\ & & 8/7 & & & -4/5 \\ & & & 9/8 & & -9/10 \\ & 0 & & & 10/9 & -1 \\ & & & & -1 & 2 \end{array}\right)$$

As our inductive hypothesis, assume we can reduce $M_n$ to $\widetilde{M}_n$ for $n \geq 1$ using row operations in the first $n+4$ rows. Recall $M_{n+1}$ contains $M_n$ as a submatrix. By the inductive hypothesis, we can row reduce the embedded matrix $M_n$ using row operations in the first $n+4$ rows of $M_{n+1}$. Since the last column of $M_{n+1}$ has zeros in the first $n+4$ entries, the last column is unaffected by these row operations. After performing the row operations, we obtain the resulting matrix, which we denote by $M'_{n+1}$, shown below.

$$M'_{n+1} = \left(\begin{array}{cccccccc} -4 & & & & & & * & 0 \\ & -7/4 & & & 0 & & * & 0 \\ & & 8/7 & & & & * & 0 \\ & & & 9/8 & & & \vdots & 0 \\ & 0 & & & \ddots & & * & \vdots \\ & & & & & \frac{n+9}{n+8} & -1 & 0 \\ & & & & & -1 & 2 & -1 \\ 0 & 0 & 0 & 0 & \cdots & 0 & -1 & 2 \end{array}\right)$$

We now perform multiple row operations. In Step A, we perform only one row operation in the second to last row, specifically $R_{n+5} \to R_{n+5} + \frac{n+8}{n+9} R_{n+4}$. In Step B, we use row operations to force the $(n+5)$th column to have zeros in the first $n+4$ entries. Notice that this will introduce values in the first $n+4$ entries in the last column and we need to use row operations only in the first $n+5$ rows. The resulting matrix is $\widetilde{M}_{n+1}$.

$$
M'_{n+1} \xrightarrow{\text{Step A}} \left(\begin{array}{cccccc|c|c}
-4 & & & & & & * & 0 \\
 & -7/4 & & & \text{\Large 0} & & * & 0 \\
 & & 8/7 & & & & * & 0 \\
 & & & 9/8 & & & \vdots & 0 \\
 & \text{\Large 0} & & & \ddots & & * & \vdots \\
\cline{7-7}
 & & & & & \frac{n+9}{n+8} & -1 & 0 \\
\cline{8-8}
 & & & & & 0 & \frac{n+10}{n+9} & -1 \\
\hline
0 & 0 & 0 & 0 & \cdots & 0 & -1 & 2
\end{array}\right)
$$

$$
\xrightarrow{\text{Step B}} \left(\begin{array}{cccccc|c|c}
-4 & & & & & & 0 & * \\
 & -7/4 & & & \text{\Large 0} & & 0 & * \\
 & & 8/7 & & & & 0 & * \\
 & & & 9/8 & & & 0 & * \\
 & \text{\Large 0} & & & \ddots & & \vdots & \vdots \\
 & & & & & \frac{n+9}{n+8} & 0 & * \\
\cline{8-8}
 & & & & & & \frac{n+10}{n+9} & -1 \\
\hline
0 & 0 & 0 & 0 & \cdots & 0 & -1 & 2
\end{array}\right)
$$

$\square$

**Lemma 2.4.** For $n = 1, 2, \ldots$, the matrix $M_n$ has signature $\sigma(M_n) = n+1$.

**Proof.** By Lemma 2.3, we can row reduce the matrix $M_n$ to $\widetilde{M_n}$ using only row operations in the first $n+4$ rows. After performing row operations as in Steps A and B shown below, we conclude $\sigma(M_n) = (n+3) - 2 = n+1$.

$$
\widetilde{M_n} \xrightarrow{\text{Step A}} \begin{pmatrix}
-4 & & & & & & * \\
 & -7/4 & & & & \text{\Large 0} & * \\
 & & 8/7 & & & & * \\
 & & & 9/8 & & & \vdots \\
 & \text{\Large 0} & & & \ddots & & * \\
 & & & & & \frac{n+9}{n+8} & -1 \\
 & & & & & 0 & \frac{n+10}{n+9}
\end{pmatrix}
$$

$$
\xrightarrow{\text{Step B}} \begin{pmatrix}
-4 & & & & & & 0 \\
 & -7/4 & & & \text{\Large 0} & & 0 \\
 & & 8/7 & & & & 0 \\
 & & & 9/8 & & & 0 \\
 & \text{\Large 0} & & & \ddots & & \vdots \\
 & & & & & \frac{n+9}{n+8} & 0 \\
 & & & & & & \frac{n+10}{n+9}
\end{pmatrix}
$$

$\square$

We are finally ready to calculate the signature of $K_n$.

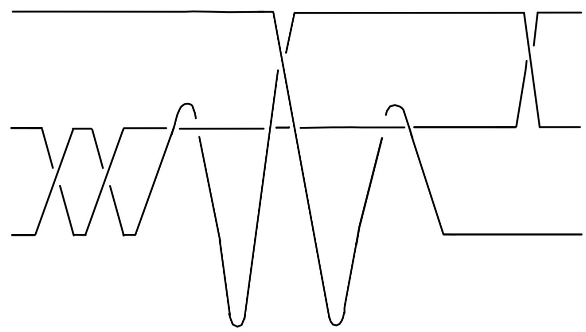

FIGURE 5. $K_1$ after isotopy

**Proposition 2.5.** For $n = 1, 2, \ldots$, the knot $K_n$ has signature $\sigma(K_n) = 2n$.

**Proof.** Recall that the Seifert matrix $V_n + V_n^T$ associated to each knot $K_n$ is the matrix $M_{2n-1}$. By Lemma 2.4, we conclude that $\sigma(K_n) = 2n$. □

**2.2. Four-ball genus of $K_n$.** The goal of this section is to calculate the four-ball genus $g_4(K_n)$. We will use Murasugi's [Mur65, Theorem 9.1] lower bound on $g_4(K_n)$ in terms of the signature of $K_n$ and directly construct a sequence of surfaces with boundary $K_n$.

**Proposition 2.6.** For each $n = 1, 2, \ldots$, the knot $K_n$ has four-ball genus $g_4(K_n) = n$.

**Proof.** We construct a surface $S_n$ in $B^4$ with $g(S_n) = n$ and $K_n$ as its boundary. We illustrate the procedure for $n = 1$. Begin with $\beta_1$ and perform braid isotopy until we arrive at Figure 5.

We create $S_1$ with $K_1$ as its boundary as seen in Figure 6. Notice that we introduced bands at each standard crossing and the remaining crossings contribute to one band with two ribbon intersections which are in green in Figure 6. To better understand this band with ribbon intersections, we have Figures 7 and 8. In Figure 7, we have colored the band to illustrate how it wraps around and through the three horizontal parallel disks. The front side of $S_1$ is highlighted in solid pink while the back side of $S_1$ is in dashed blue. The two ribbon intersections are still highlighted in green. The three disks in the left sketch of Figure 8 that are colored pink, yellow, and dark blue (from top to bottom) appear as line segments of the right sketch when viewed from the right hand side. The band begins at the black dot on the pink disk, creates two ribbon intersections via passing through the blue and then yellow disks, and ends at the black dot on the blue disk. We now push a neighborhood of the ribbon intersections, which is highlighted in blue in Figure 6, into the 4-ball. This resolves the ribbon intersection and the resulting surface, which we call $S_1$, is properly embedded in $B^4$.

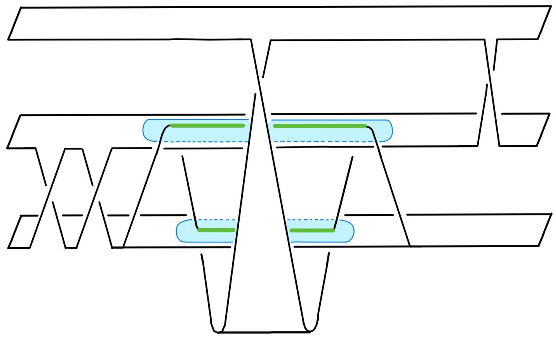

FIGURE 6. $S_1$ with ribbon intersections

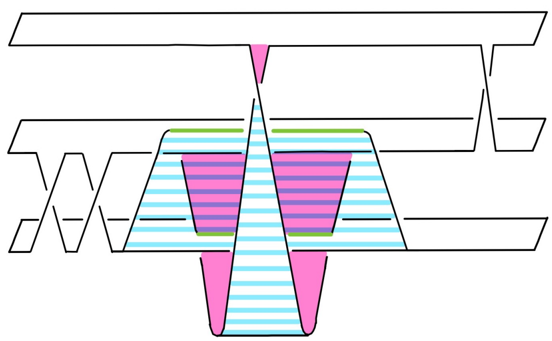

FIGURE 7. $S_1$ with colored band

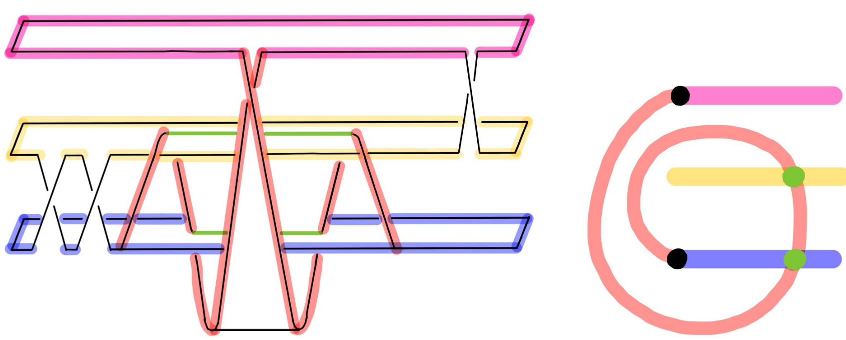

FIGURE 8. Band in $S_1$

We calculate the Euler characteristic of $S_1$ using the fact that there are three disks and four bands.

$$\chi(S_1) = 3 - 4 = -1.$$

Since $\chi(S) = 1 - 2g(S)$ for knots, we have that $g(S_1) = 1$.

We can create a surface $S_n$ with $K_n$ as its boundary by simply having $2n$ negative bands instead of the two negative bands we have on the left in $S_1$. Again we resolve the ribbon intersections and $S_n$ is a properly embedded smooth surface in $B^4$.

Thus, $S_n$ has a total of $2n+2$ bands comprising of the $2n$ negative bands on the left of the surface, the large band that has two ribbon intersections, and one positive band on the right of the surface. We calculate the Euler characteristic of the surface $S_n$

$$\chi(S_n) = 3 - (2n+2) = 1 - 2n$$

and we have that $g(S_n) = n$. Hence, $g_4(K_n) \leq n$.

K. Murasugi proved that $\frac{1}{2}|\sigma(K)| \leq g_4(K)$ in [Mur65, Theorem 9.1]. By Proposition 2.5, we have that $\frac{1}{2}(2n) \leq g_4(K_n)$. Hence, $g_4(K_n) = n$. $\square$

**Corollary 2.7.** For each $n = 1, 2, \ldots$, the defect $\delta_4(K_n) = 2n$. In particular, $K_n$ is non-quasipositive.

**Proof.** We compute the self-linking number of braids $\beta_n$ in our sequence and obtain:

$$sl(\widehat{\beta}_n) = -3 + 5 - (2n+3) = -2n - 1.$$

By the generalized Jones conjecture [DP13, LM14, Kaw06], the maximal self-linking number is realized at the minimal braid index. As the braid index of $K_n$ is 3 and $\beta_n$ is a 3-braid, we obtain

$$SL(K_n) = sl(\widehat{\beta}_n) = -2n - 1.$$

By Proposition 2.6 we have $g_4(K_n) = n$. We compute the defect

$$\delta_4(K_n) = \frac{1}{2}(2g_4(K_n) - 1 - SL(K_n)) = 2n.$$

By Proposition 1.5 we conclude that $K_n$ is non-quasipositive. $\square$

**2.3. The $s$ invariant of $K_n$.** The goal of this section is to calculate the $s$ invariant of $K_n$. We will determine the Murasugi's form [Mur74] of the braid $\beta_n$. Then we use it to calculate the $s$ invariant for $K_n$.

**Lemma 2.8.** For $n = 1, 2, \ldots$, the braid $\beta_n$ is conjugate to the braid

$$A_n = (\sigma_1\sigma_2)^3\sigma_1(\sigma_2^{-1})^{2n+5}$$

that belongs to the first type in the Murasugi classification of 3-braids [Mur74].

**Proof.** We begin by examining the braid $A_n = (\sigma_1\sigma_2)^3\sigma_1(\sigma_2^{-1})^{2n+5}$ depicted at the top of Figure 9. Note that the box labeled $T$ contains $2n+2$ negative twists, or $2n+2$ $\sigma_2^{-1}$'s throughout the figure. Using conjugation, we are able to move the negative crossing highlighted in blue along $\sigma_1$ and $\sigma_2$ to cancel with a $\sigma_1$. Similarly, we can move the negative crossing highlighted in pink underneath $\sigma_1$ and $\sigma_2$ to cancel with another $\sigma_1$. The last braid is conjugate to $\beta_n$ and we are done. $\square$

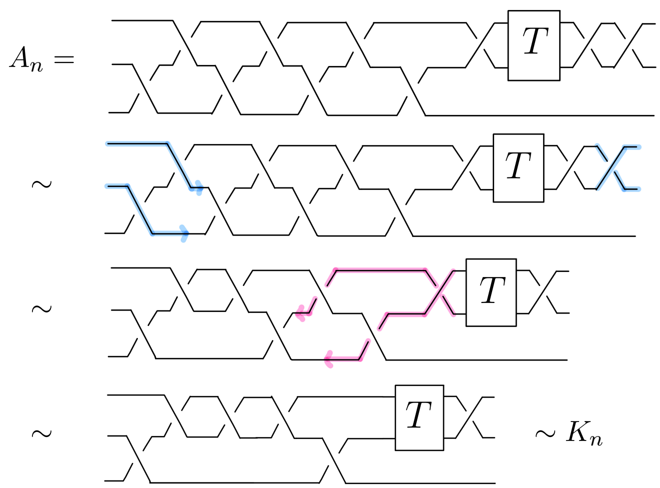


FIGURE 9. $K_n$ is conjugate to $A_n$

**Proposition 2.9.** For $n = 1, 2, \ldots$, $s(K_n) = -2n$; thus, $\delta_s(K_n) = 0$.

**Proof.** By Lemma 2.8, we know that $A_n$ is of Type 1 according to Murasugi's classification of 3-braids with $d = 1$ and $a_1 = 2n + 5$ [Mur74]. By Martin [Mar19, Theorem 4.1], since $\beta_n$ is conjugate to $A_n$ which is of Type 1 with $d > 0$ and some $a_i > 0$, we have that $s(K_n) = w(K_n) - 2$ where $w$ denotes the writhe of the knot. Recall that the writhe is the number of positive crossings minus the number of negative crossings in the knot diagram. Hence

$$w(K_n) = 7 - (2n + 5) = -2n + 2.$$

We conclude that

$$s(K_n) = -2n + 2 - 2 = -2n.$$

$\square$

**2.4. The $\boldsymbol{\tau}$ invariant of $\boldsymbol{K_n}$.** We will show that the $\tau$-defect $\delta_\tau$ vanishes for each knot $K_n$.

**Proposition 2.10.** For $n = 1, 2, \ldots$, the $\tau$ invariant of $K_n$ is $\tau(K_n) = -n$.

**Proof.** We perform a crossing change on the rightmost crossing of $K_n$ to obtain a knot $P_n$, as shown in Figure 10 for $n = 1$. After doing a Reidemeister I move, and two Reidemeister II moves, we see that the knot $P_n$ is the $(2, -(2n+1))$–torus knot $T_{2,-(2n+1)}$. This sequence of isotopies is illustrated in Figure 11. Recall that $\tau$ invariant satisfies the crossing change inequality [OS03, Corollary 1.5]

$$0 \leq \tau(K_n) - \tau(T_{2,-(2n+1)}) \leq 1.$$

Since $\tau(T_{2,-(2n+1)}) = -n$, we have $-n \leq \tau(K_n) \leq -n + 1$.

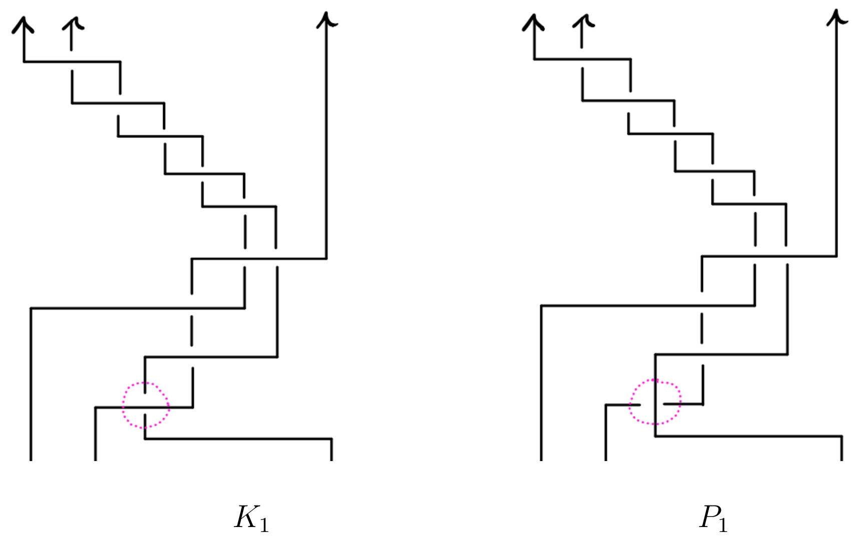


FIGURE 10. The knot $K_1$ is the closure of the braid shown on the left. After a crossing change, we obtain the knot $P_1$ as the closure of the braid shown on the right.

Next, we may change a negative crossing in $K_n$ to a positive crossing to get a knot $R_n$ satisfying

$$\tau(K_n) \leq \tau(R_n)$$

by the crossing change inequality. We may then change a positive crossing in $R_n$ to a negative crossing to obtain the torus knot $T_{2,-(2n+3)}$. This process is illustrated in Figure 12. We have

$$\tau(R_n) \leq \tau(T_{2,-(2n+3)}) + 1 = -n.$$

Thus, we have $\tau(K_n) \leq -n$. Together with the first step, we find that $\tau(K_n) = -n$ for each positive integer $n$. □

**2.5. The transverse and contact invariants of $K_n$.** This section is dedicated to exploring invariants in the literature that can be used to detect if a knot is non-quasipositive. We study the Ozsváth-Szabó-Thurston transverse invariant $\hat{\theta}(K)$ from knot Floer homology [OST08] and Plamenevskaya's transverse invariant $\psi(K)$ from Khovanov homology [Pla06]. Recall that for quasipositive knots, the transverse invariants $\psi(K)$ and $\hat{\theta}(K)$ are both nonzero by [Pla18]. Each knot $K_n$ is non-quasipositive by Corollary 2.7. However, the propositions below show that the non-quasipositive property of the knots $K_n$ is not detected by $\hat{\theta}(K)$ and $\psi(K)$.

**Proposition 2.11.** For all $n \geq 1$, the invariant $\psi(K_n)$ is nonzero.

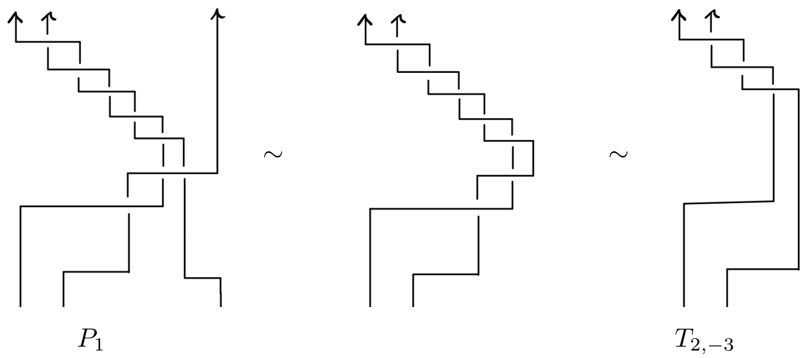


FIGURE 11. The knot $P_1$ is isotopic to the torus knot $T_{2,-3}$. The leftmost picture shows the knot $P_1$ after a Reidemeister II move. Perform a Reidemeister I move to obtain the knot in the center picture. Finally, perform two Reidemeister II moves to obtain $T_{2,-3}$ shown in the rightmost picture.

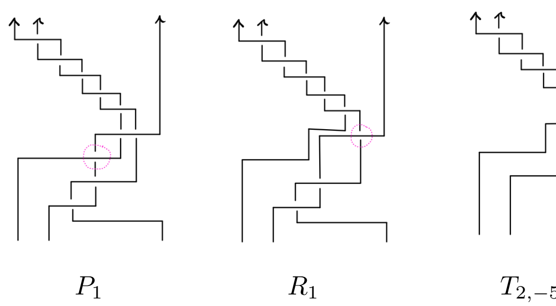


FIGURE 12. The knot $P_n$ is a single crossing change away from the knot $R_n$. The knot $R_n$ is a single crossing change away from the torus knot $T_{2,-(2n+3)}$. The illustrations are shown for $n = 1$. Note that the crossing changes and Reidemeister moves occur away from the twisting region specified by $n$.

**Proof.** In [Mar19, Proposition 2.10], Martin proved that for any $m$-braid $\beta$, if $s(\hat{\beta}) - 1 = w(\beta) - m$ then $\psi(\hat{\beta}) \neq 0$. In the proof of Proposition 2.9, we showed that $s(K_n) = w(K_n) - 2$, which satisfies Martin's condition. Therefore, $\psi(K_n) \neq 0$. $\square$

**Proposition 2.12.** For all $n \geq 1$, the invariant $\hat{\theta}(K_n)$ is nonzero.

**Proof.** By Proposition 2.9, we know that $sl(K_n) = s(K_n) - 1$. By [Pla18, Proposition 3.2] the knot $K_n$ is right-veering for all $n$. Furthermore, by [Pla18, Theorem 1.2], $\hat{\theta}(K_n) \neq 0$ for all $n$. $\square$

Recall that the double cover of $S^3$ branched over a transverse link $L$ carries a natural contact structure $\xi_L$ lifted from $(S^3, \xi_{\mathrm{std}})$.

**Corollary 2.13.** Let $(\Sigma(K_n), \xi_{K_n})$ be the double cover of $(S^3, \xi_{\mathrm{std}})$ branched over the transverse knot $K_n$. For $n = 1, 2, \ldots,$ the Heegaard Floer contact invariant $c(\xi_{K_n})$ does not vanish.

**Proof.** By [Pla18, Corollary 4.2], since $\hat{\theta}(K_n) \neq 0$, the Heegaard Floer contact invariant $c(\xi_{K_n}) \neq 0$. □

## References


[Ben83] Bennequin, Daniel. Entrelacements et équations de Pfaff. *Third Schnepfenried geometry conference, Vol. 1* (Schnepfenried, 1982), 87–161, Astérisque, 107–108. *Soc. Math. France, Paris*, 1983. MR0753131 (81d:57034), Zbl 0516.00018. 125

[DP13] Dynnikov, Ivan A.; Prasolov, Maxim V. Bypasses for rectangular diagrams. A proof of the Jones conjecture and related questions. *Trans. Moscow Math. Soc.* **2013**, 97-144. MR3235791, Zbl 1307.57004, doi: 10.1090/S0077-1554-2014-00210-7. 135

[HIK19] Hamer, Jesse; Ito, Tetsuya; Kawamuro, Keiko. Positivities of knots and links and the defect of Bennequin inequality. *Experimental Journal of Mathematics*, 2019. doi: 10.1080/10586458.2019.1596848. 125, 126

[Hed10] Hedden, Matthew. Notions of positivity and the Ozsváth-Szabó concordance invariant. *J. Knot Theory Ramifications* **19** (2010), no. 5, 617–629. MR2646650, Zbl 1195.57029, doi: 10.1142/S0218216510008017. 126

[Kaw06] Kawamuro, Keiko. The algebraic crossing number and the braid index of knots and links. *Algebr. Geom. Topol.* **6** (2006), 2313–2350. MR2286028, Zbl 1128.57007, arXiv:0907.1019, doi: 10.2140/agt.2006.6.2313. 135

[Kaw07] Kawamura, Tomomi. The Rasmussen invariants and the sharper slice-Bennequin inequality on knots. *Topology* **46** (2007), no. 1, 29–38. MR2288725, Zbl 1114.57010, doi: 10.1016/j.top.2006.10.001. 125

[LM14] LaFountain, Douglas J.; Menasco, William W. Embedded annuli and Jones' conjecture. *Algebr. Geom. Topol.* **14** (2014), no. 6, 3589–3601. MR3302972, Zbl 1336.57012, arXiv:1302.1247, doi: 10.2140/agt.2014.14.3589. 135

[Mar19] Martin, Gage. Annular Rasmussen invariants: Properties and 3-braid classification. Preprint, 2019. arXiv:1909.09245. 136, 138

[Mur65] Murasugi, Kunio. On a certain numerical invariant of link types. *Trans. Amer. Math. Soc.* **117** (1965), 387–422. MR0171275, Zbl 0137.17903, doi: 10.2307/1994215. 133, 135

[Mur74] Murasugi, Kunio. On closed 3-braids. Memoirs of the American Mathmatical Society, 151. *American Mathematical Society, Providence, R.I.*, 1974. vi+114 pp. MR0356023, Zbl 0327.55001, doi: 10.1090/memo/0151. 135, 136

[OS03] Ozsváth, Peter; Szabó, Zoltán. Knot Floer homology and the four-ball genus. *Geom. Topol.* **7** (2003), 615–639. MR2026543, Zbl 1037.57027, arXiv:math/0301149, doi: 10.2140/gt.2003.7.615. 125, 136

[OST08] Ozsváth, Peter; Szabó, Zoltán; Thurston, Dylan. Legendrian knots, transverse knots and combinatorial Floer homology. *Geom. Topol.* **12** (2008), no. 2, 941–980. MR2403802, Zbl 1144.57012, arXiv:math/0611841, doi: 10.2140/gt.2008.12.941. 125, 126, 137

[Par12] Pardon, John. The link concordance invariant from Lee homology. *Algebr. Geom. Topol.* **12** (2012), no. 2, 1081–1098. MR2928905, Zbl 1263.57007, arXiv:1107.4702, doi: 10.2140/agt.2012.12.1081. 125

[Pla04] Plamenevskaya, Olga. Bounds for the Thurston–Bennequin number from Floer homology. *Algebr. Geom. Topol.* **4** (2004), 399–406. MR2077671, Zbl 1070.57014, arXiv:math/0311090, doi: 10.2140/agt.2004.4.399. 125, 126

[Pla06] Plamenevskaya, Olga. Transverse knots and Khovanov homology. *Math. Res. Lett.* **13** (2006), no. 4, 571–586. MR2250492, Zbl 1143.57006, arXiv:math/0412184, doi: 10.4310/MRL.2006.v13.n4.a7. 125, 126, 137

[Pla18] Plamenevskaya, Olga. Braid monodromy, orderings and transverse invariants. *Algebr. Geom. Topol.* **18** (2018), no. 6, 3691–3718. MR3868232, Zbl 1408.57016, doi: 10.2140/agt.2018.18.3691. 137, 138, 139

[Ras10] Rasmussen, Jacob. Khovanov homology and the slice genus. *Invent. Math.* **182** (2010), no. 2, 419–447. MR2729272, Zbl 1211.57009, arXiv:math/0402131, doi: 10.1007/s00222-010-0275-6. 125

[Rud93] Rudolph, Lee. Quasipositivity as an obstruction to sliceness. *Bull. Amer. Math. Soc.* (N.S.) **29** (1993), no. 1, 51–59. MR1193540, Zbl 0789.57004, arXiv:math/9307233, doi: 10.1090/S0273-0979-1993-00397-5. 125

[Shu07] Shumakovitch, Alexander N. Rasmussen invariant, slice-Bennequin inequality, and sliceness of knots. *J. Knot Theory Ramifications* **16** (2007), no. 10, 1403–1412. MR2384833, Zbl 1148.57011, arXiv:math/0411643, doi: 10.1142/S0218216507005889. 125, 126

(Elaina Aceves) Department of Mathematics, University of Iowa, Iowa City, IA 52242, USA
elaina-aceves@uiowa.edu

(Keiko Kawamuro) Department of Mathematics, University of Iowa, Iowa City, IA 52242, USA
keiko-kawamuro@uiowa.edu

(Linh Truong) Department of Mathematics, University of Michigan, Ann Arbor, MI 48103, USA
tlinh@umich.edu

This paper is available via http://nyjm.albany.edu/j/2021/27-4.html.